Korean Journal of Radiology

KJR

Feasibility of Novel Three-Dimensional Magnetic Resonance Fingerprinting of the Prostate Gland: Phantom and Clinical Studies

Dongyeob Han[1], Moon Hyung Choi[2], Young Joon Lee[2], Dong-Hyun Kim[3]

[1]Siemens Healthineers Ltd., Seoul, Korea; [2]Department of Radiology, Eunpyeong St. Mary's Hospital, College of Medicine, The Catholic University of Korea, Seoul, Korea; [3]School of Electrical and Electronic Engineering, Yonsei University, Seoul, Korea

Objective: To evaluate the feasibility of a new three-dimensional (3D) MR fingerprinting (MRF) technique for the prostate gland by conducting phantom and clinical studies.
Materials and Methods: The new 3D MRF technique used in this study enables quick data acquisition and has a high resolution. For the phantom study, the MRF T1 and T2 values in an in-house phantom were compared with those of gold-standard mapping methods using linear regression analysis. For the clinical study, we evaluated 90 patients who underwent prostate imaging with MRF for suspected prostate cancer between September 2019 and February 2020. The mean T1 and T2 values were compared in the peripheral zone, transition zone, and focal lesions using paired t tests. The differences in the T1 and T2 values according to cancer aggressiveness were evaluated using one-way analysis of variance.
Results: In the phantom study, the MRF T1 and T2 values showed a perfect correlation with the gold-standard T1 and T2 values (R > 0.99). In the clinical study, the T1 and T2 values in the peripheral zone were significantly higher than those in the transitional zone ($p < 0.001$, both). The T1 and T2 values in prostate cancer were significantly lower than those in the peripheral and transitional zones. The higher the grade of cancer, the lower the T2 values.
Conclusion: The T1 and T2 values obtained from the 3D MRF showed a perfect correlation with the gold standard values in the phantom study. Differences in the T1 and T2 values among the different zones of the prostate gland were identified using 3D MRF in patients.
Keywords: *Magnetic resonance imaging; Fingerprinting; Prostate gland; T1 relaxation time; T2 relaxation time*

INTRODUCTION

The benefit of prostate MRI over transrectal ultrasound-guided biopsy in the diagnosis of clinically significant prostate cancer is well-established [1,2]. Prostate cancer

shows hypointensity on T2-weighted images (T2WI) compared to normal prostate tissue. However, the relatively low signal intensity of prostate cancer cannot be measured quantitatively. In conventional T1- and T2WI, signal intensities may vary due to many factors, such as the type of scanners or coils, and parameters. Therefore, T1 or T2 mapping is necessary for the quantification of T1 and T2 values to obtain the objective parameters. Previous studies on T1 or T2 maps have shown promising results in differentiating prostate cancer from normal tissue and in determining the aggressiveness of prostate cancers [3-9]. However, the length of time needed to acquire T1 and T2 maps hinders their clinical use, and these maps cannot replace the conventional T1- and T2WI.

MR fingerprinting (MRF) is a technique that utilizes a completely different concept of data acquisition from conventional MRI [8]. In conventional MRI, data are

acquired repeatedly with constant parameters. On the other hand, signals are obtained in MRF by using various acquisition parameters in a pseudorandom manner. The acquired MRF data are highly undersampled compared with conventional data, but the signals from different tissues have unique patterns. A pattern recognition algorithm is applied to match the unique signal, the so-called fingerprint, to a predefined dictionary containing signal evolutions from all possible combinations of parameters. The T1 and T2 values of the corresponding signal from the dictionary were assigned as T1 and T2 values of the pixel. Therefore, T1 and T2 values can be simultaneously acquired from MRF faster than from conventional T1 and T2 maps.

Several prostate MRF studies have shown that the T1 and T2 values are significantly different between prostate cancer and normal prostate tissue. Additionally, T1 and T2 MRF correlate well with the histological aggressiveness of prostate cancer in both the peripheral and transition zones [10-12]. In a recent study, significant associations were found between MRF-based parameters and the tissue compartment ratio (epithelium, stroma, and lumen) based on histopathology [13]. MRF appears to have great potential as a quantitative parameter in prostate imaging. However, the MRF in previous studies used a two-dimensional (2D) data acquisition method and obtained images with moderate spatial resolution (1 x 1 mm) and a large thickness (5 mm slice thickness) in a relatively long acquisition time. Therefore, we applied the new three-dimensional (3D) MRF technique to obtain MRF images with better spatial resolution and shorter acquisition time.

The purpose of this study was to evaluate the feasibility of the new 3D MRF technique in the prostate gland using phantom and clinical studies.

MATERIALS AND METHODS

MRF and MRI Protocol

We used 3D MRF with hybrid radial-echo-planar imaging (EPI) trajectory for both phantom and clinical studies. The 3D MRF collects k-space data using radial acquisition in the kxy domain while applying EPI acquisition in the slice encoding direction (k_z). Furthermore, the k-t acceleration was applied through the slice encoding direction similar to the acceleration with previous 3D MRF [14], to reduce the scan time. Iterative reconstruction using conjugate gradient sensitivity encoding (CG-SENSE) was also applied to improve the image quality. Therefore, this method allows acquisition of high-resolution 3D quantitative maps within practical scan times. MRF parameters are summarized in the Supplement.

Multiparametric (mp) MRI was performed for the clinical study, which included three-plane T2WI, axial T1WI, diffusion-weighted images, and dynamic contrast-enhanced images. Endorectal coils were not used in any patient. Detailed parameters are listed in Table 1. The total acquisition time for mpMRI and MRF was approximately 23 minutes. All examinations were performed using a 3T system (Magnetom Vida, Siemens Healthineers) with a 30-channel surface coil and a 64-channel or 128-channel spine coil.

Phantom Study

We created an in-house phantom to compare the T1 and T2 values between MRF-derived T1 and T2 maps and conventional T1 and T2 maps. The phantom was made

Table 1. Image Acquisition Parameters

	T2WI (TSE)	T1WI (TSE)	DWI	MRF	DCEI (GRASP)
TR, ms	2500–3000	500–700	5200–6000	16	4
TE, ms	103	9	76	4	2
Field of views, mm	180 x 180	180 x 180	200 x 180	160 x 160	200 x 200
Matrix	320 x 320	320 x 320	120 x 108		224 x 224
Resolution, mm	0.6 x 0.6	0.6 x 0.6	1.7 x 1.7	0.6 x 0.6	0.9 x 0.9
Flip angle, °	136	120	90		12
Slice thickness, mm	3	3	3	3	3
Gap	0	0	0		0
NEX	2	2	2, 2, 9, 9		1
b values, s/mm²	-	-	0, 100, 1000, 1500	-	-
Acquisition time, min:sec	3:32	3:35	6:18	3:48	5:40

DCEI = dynamic contrast-enhanced image, DWI = diffusion-weighted image, GRASP = Golden-angle RAdial Sparse Parallel MRI, MRF = MR fingerprinting, NEX = number of excitation, TE = echo time, TR = repetition time, TSE = turbo spin echo, T1WI = T1-weighted image, T2WI = T2-weighted image

of nine tubes with varying concentrations of manganese chloride ($MnCl_2$) mixed with distilled water (10, 20, 30, 40, 50, 60, 70, 100, 150, and 200 µM).

A gold-standard T1 map was obtained with 2D multiple inversion recovery spin echo (SE) MRI (inversion time [TI] set: [50, 100, 200, 400, 800, 1200, 1600, 2400, 4800] ms, repetition time [TR] = 10 seconds, resolution: 1 x 1 mm^2 (2 x interpolated), slice thickness = 2 mm, field of view (FOV) = 128 x 128 mm^2, scan time for each SE: 10 minutes 52 seconds, total scan time for nine different TI SEs: 1 hour 38 minutes). For a gold-standard T2 map, 2D multiple echo time (TE) SE MRI was acquired (TE set: [10, 20, 40, 60, 100, 150, 200, 400, 800] ms, TR = 10 seconds, resolution: 1 x 1 mm^2 (2 x interpolated), slice thickness = 2 mm, FOV = 128 x 128 mm^2, scan time for each SE: 10 minutes 52 seconds, total scan time (9 different TI SEs): 1 hour 38 minutes. Mono-exponential fitting was performed for the gold standard T1 and T2 maps.

Patient

This retrospective study was approved by our Institutional Review Board, and the requirement for informed consent was waived (IRB No. PC20RISI0059).

Patients who underwent prostate MRI between September 2019 and February 2020 were eligible for the study. The exclusion criteria were 1) no MRF done, 2) prostatectomy before MRI examination, 3) transurethral resection of the prostate gland before MRI, 4) no normal prostate gland tissue, and 5) previously diagnosed prostate cancer. A total of 90 patients were included in this study. The inclusion process is summarized in Figure 1. The age, level of prostate-specific antigen (PSA), prostate biopsy, or prostatectomy results were collected from the electronic medical records.
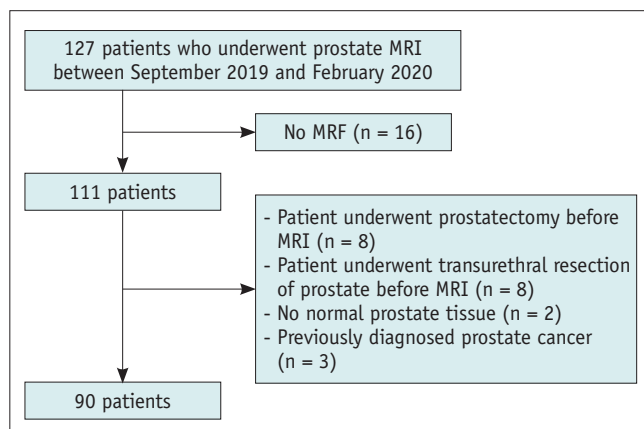
Fig. 1. Flowchart of patient inclusion. MRF = MR fingerprinting

Image Analysis

A radiologist with 10 years of experience in prostate MRI reviewed the mpMRI examinations and assigned the Prostate Imaging-Reporting and Data System v2.1 classification. If there were multiple prostate cancers detected, each lesion was classified according to PI-RADS v2.1. The radiologist recorded the location and size of the lesions, and captured the image containing the largest area of each lesion.

The same radiologist analyzed the MRF images using ITK-SNAP version 3.8.0 (www.itksnap.org) [15]. The radiologist loaded the T1 and T2 maps into the software simultaneously, selected the section with the largest area of normal-appearing prostate gland tissue and drew regions of interest (ROIs) that covered the entire peripheral zone and transition zone, respectively, in all cases. For patients with focal lesion with a PI-RADS score of 3 or higher, an ROI is drawn on the section in which the largest area of the tumor was seen. ROIs were drawn with reference to mpMRI. If there were multiple lesions in a patient, the lesion with the highest PI-RADS score or the largest lesion with the same PI-RADS score was chosen for analysis. We obtained the averages and standard deviations (SDs) of the T1 and T2 values from the ROIs on both maps. Figure 2 shows the images of a representative case.

Biopsy and Pathology Correlation

Biopsy was performed in patients with focal lesions on mpMRI or who had high risk of prostate cancer even with negative prostate MRI results. Four patients with focal lesions with PI-RADS score of 4 or higher did not undergo prostate biopsy. Transrectal ultrasound-guided biopsy was performed by one of two genitourinary radiologists with 6 and 18 years of experience in prostate biopsy MRI-ultrasound fusion. The prostate cancer was classified according to the Gleason grade. Pathology results correlated with focal lesions detected on MRI. If radical prostatectomy was performed in a patient, prostatectomy results, rather than biopsy results, were used for analysis. If prostate cancer was not pathologically confirmed by targeted biopsy of the focal lesion, the lesion was classified as non-cancerous.

Statistical Analysis

In the phantom study, the similarity in the T1 and T2 values between 3D MRF, and the gold standards was compared using linear regression analysis and Pearson's correlation coefficient.

The patients' characteristics were summarized using the mean and SD, range for continuous values, and the proportion for categorical values. The Kolmogorov-Smirnov test was used to evaluate whether the data were normally distributed. In all cases, the T1 and T2 values were compared between the peripheral and transitional zones using paired t tests. In patients who had focal lesion on MRI and underwent biopsy, the T1 and T2 values were
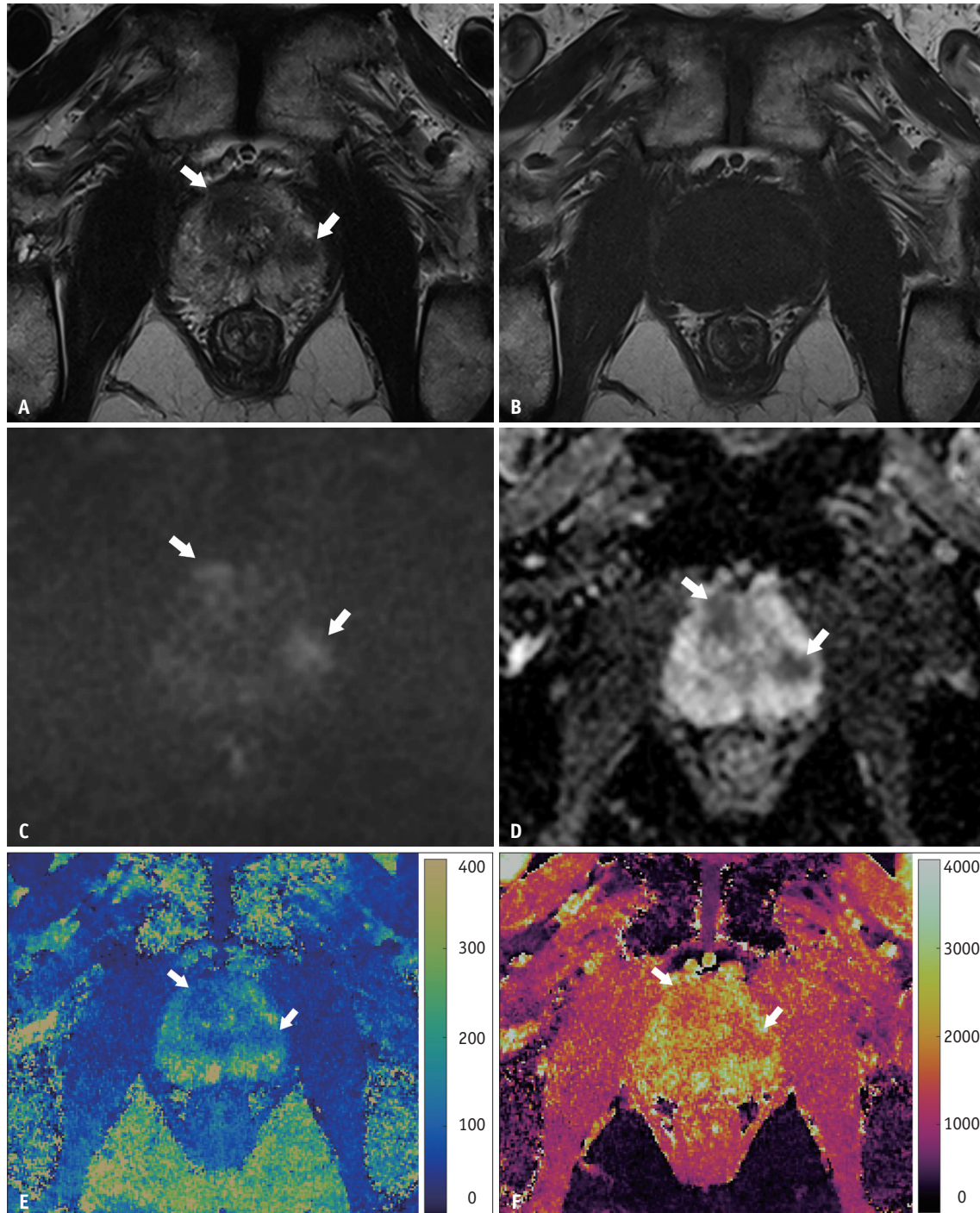
Fig. 2. A 69-year-old male with elevated prostate-specific antigen (7.31 ng/mL) underwent prostate MRI.
A-F. Two lesions in the Rt transition zone and Lt peripheral zone show low signal intensity on T2-weighted images **(A)**, iso-signal intensity on T1-weighted images **(B)**, high signal intensity on diffusion-weighted images **(C)**, and low values on apparent diffusion coefficient maps **(D)**. They show lower values on both the MR fingerprinting-derived T2 map **(E)** and T1 map **(F)**. The lesions (arrows) were confirmed as prostate cancer: right lesion Gleason 9 (4 + 5) and left lesion Gleason 7 (3 + 4).

compared among the peripheral zone, transition zone, and focal lesion using paired *t* tests. The parameters measured in the focal lesion of patients who did not undergo biopsy were discarded. Pearson correlation tests were applied to investigate the correlation between T1 or T2 values and Gleason grade groups. One-way ANOVA was used to compare the T1 and T2 values among the pathology results (noncancer, Gleason grade groups 1, 2–3, and 4–5) because the T1 and T2 values were normally distributed. Statistical analysis was performed using SPSS software (version 24.0; IBM Corp.).

RESULTS

Phantom Study

The relationship between the T1 value from MRF and the gold standard is summarized in the fitted regression line (Fig. 3A) with the following equation: gold-standard T1 value = 0.98 x MRF T1 value - 57. The regression equation for the T2 value was as follows: gold-standard T2 relaxation time = 1 x MRF T2 value + 13 (Fig. 3B). The correlation coefficients between MRF and the gold standard were 0.99979 and 0.99810 for the T1 and T2 values, respectively.

Clinical Study

Among the 90 patients (mean age ± SD, 69 ± 8.5 years;

range, 43–89 years), 45 underwent biopsy and 25 (27.8%) were diagnosed with prostate cancer. The mean PSA level was 19.3 ng/mL. Seven patients underwent radical prostatectomy. The patient characteristics are summarized in Table 2.

In all cases, the T1 and T2 values in the peripheral zone were significantly higher than those in the transitional zone ($p < 0.001$, both) (Table 3). In patients with pathologically confirmed prostate cancer, the mean ± SD of T1 value in prostate cancer was 1557.8 ± 289.1 ms, which was significantly lower than that in the peripheral and transition zones ($p = 0.002$ and $p = 0.030$, respectively). The mean ± SD of T2 value in prostate cancer (98.4 ± 16.8) was also significantly lower than the values in the peripheral and transition zones ($p < 0.001$, both).

Among the 90 patients, there were focal lesions with biopsy results in 29 patients. Prostate cancer was not seen in 4 out of the 29 patients. The T2 value was significantly correlated with the Gleason grade group ($r = -0.443$, $p = 0.034$), and the T1 values were not correlated with the Gleason grade group ($r = -0.168$, $p = 0.444$). The T2 values were lower in cancers with higher Gleason grade (Fig. 4A). The mean ± SD of T2 values in the non-cancers (140.7 ± 18.5 ms) were significantly higher than that in the Gleason grade groups 2–3 lesions (97.7 ± 17.2 ms) and groups 4–5 lesions (90.7 ± 9.5 msec). Although the T2 values in
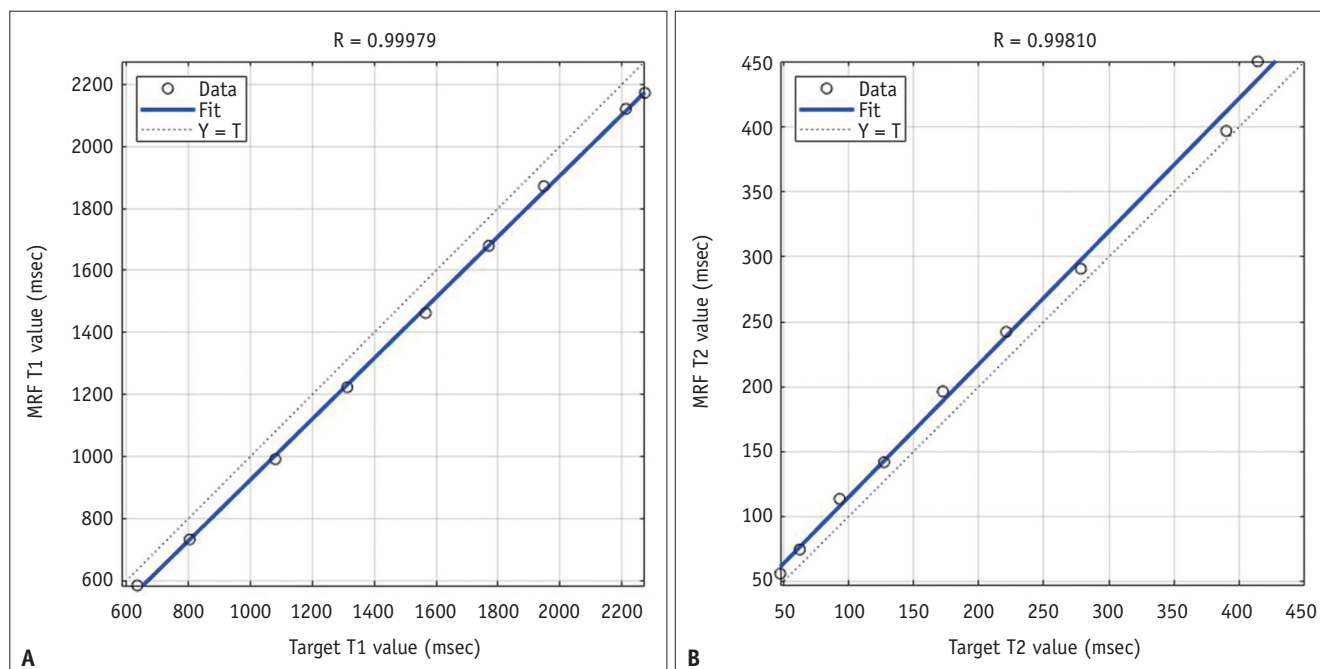
Fig. 3. Results of the phantom study.
A, B. The MRI-derived T1 value **(A)** and T2 value **(B)** show perfect correlation with the target values obtained from the gold-standard mapping methods. MRF = MR fingerprinting

Gleason grade group 1 lesions (117.7 ± 14.9 ms) were lower than that in the non-cancers, no significant difference was found (*p* = 0.347). The T1 values were not significantly different according to pathology results (Fig. 4B).

DISCUSSION

Several studies have shown meaningful results of MRF in providing objective parameters to differentiate prostate cancer from normal prostate tissue [10-13]. The MRF protocol used in previous studies can take approximately 7–8 minutes to acquire images from the entire prostate gland. Our study shows that a new 3D MRF technique is feasible

for the prostate gland. The new 3D MRF technique allowed us to obtain prostate images with a shorter acquisition time (3 minutes 48 seconds) than the protocol used in previous studies. The accuracy of the T1 and T2 values from the MRF was verified the values from the conventional mapping methods in the phantom study. Additionally, the results from the clinical study showed different values for the peripheral zone, transition zone, and focal lesion.

The T1 and T2 values from the MRF of the peripheral zone were significantly higher than those in the transition zone. In patients who underwent biopsy, prostate cancer had significantly lower T1 and T2 values in both the peripheral and transition zones. In our study, the higher the aggressiveness of prostate cancer, the lower the T2 value. The mean T2 value in the non-cancer areas was significantly higher than that in prostate cancers with Gleason grades 2–3 and 4–5. Similar results have been observed in the transition zone and peripheral zone separately in previous studies [10-12]. Although a previous study using the transition zone showed the usefulness of T1 values in differentiating prostate cancer from non-cancer areas, there was no significant difference seen in the T1 value between non-cancer and prostate cancer or among prostate cancers with different Gleason grade groups in this study. The differences in the results may be caused by the location of the prostate focal lesions or the small number of patients who underwent biopsy in our study.

In this study, the average T1 values in the peripheral zone and transition zone were 1875.7 msec and 1689.4 msec, respectively. In a study that used inversion recovery sequence at 3T MRI, the T1 values in the peripheral zone and transition zone in the mid-gland were 1756 and 1503 ms, respectively [3]. MRF studies reported T1 values of 2240 and 1800 ms in the peripheral zone and transition zone, respectively [10,11]. In our study, the average T2 values in the peripheral and transition zones were 173.4 and 121.4 ms, respectively. On the other hand, the T2 values in the peripheral zone in previous studies varies from 149 ms to 211 ms by conventional T2 mapping techniques on 3T MRI [5,16,17]. In previous MRF studies, the T2

Table 2. Patients' Characteristics

Characteristic	Value
Number of patients	90
Age, year, mean ± SD	69.9 ± 8.5 (range, 43–89)
Prostate specific antigen, ng/mL, mean ± SD	19.3 ± 59.2 (range, 1.38–421.3)
Number of focal lesions/patient	
No lesion	56 (62.2)
One	25 (27.8)
Two	6 (6.7)
Three	3 (3.3)
PI-RADS score of the index lesion	
PI-RADS 1	56 (62.2)
PI-RADS 2	2 (2.2)
PI-RADS 3	1 (1.1)
PI-RADS 4	15 (16.7)
PI-RADS 5	16 (17.8)
Patients who underwent biopsy	45
Lesions ≤ PI-RADS 2 on MRI	16 (35.6)
Lesions ≥ PI-RADS 3 on MRI	29 (64.4)
Prostate cancer	25
Gleason grade group 1	3 (12.0)
Gleason grade group 2	15 (60.0)
Gleason grade group 3	1 (4.0)
Gleason grade group 4	3 (12.0)
Gleason grade group 5	3 (12.0)

Data are number of patients with % in each characteristic in parentheses unless specified otherwise. PI-RADS = Prostate Imaging-Reporting and Data System, SD = standard deviation

Table 3. MR Fingerprinting-Derived T1 and T2 Values in PZ and TZ

	PZ	TZ	Prostate Cancer	*P*		
				PZ vs. TZ	PZ vs. Cancer	TZ vs. Cancer
T1 value, msec	1875.7 ± 323.2	1689.4 ± 220.6	1557.8 ± 289.1	< 0.001	0.002	0.030
T2 value, msec	173.4 ± 50.7	121.4 ± 19.7	98.4 ± 16.8	< 0.001	< 0.001	< 0.001

Data are mean ± standard deviation. PZ = peripheral zone, TZ = transition zone
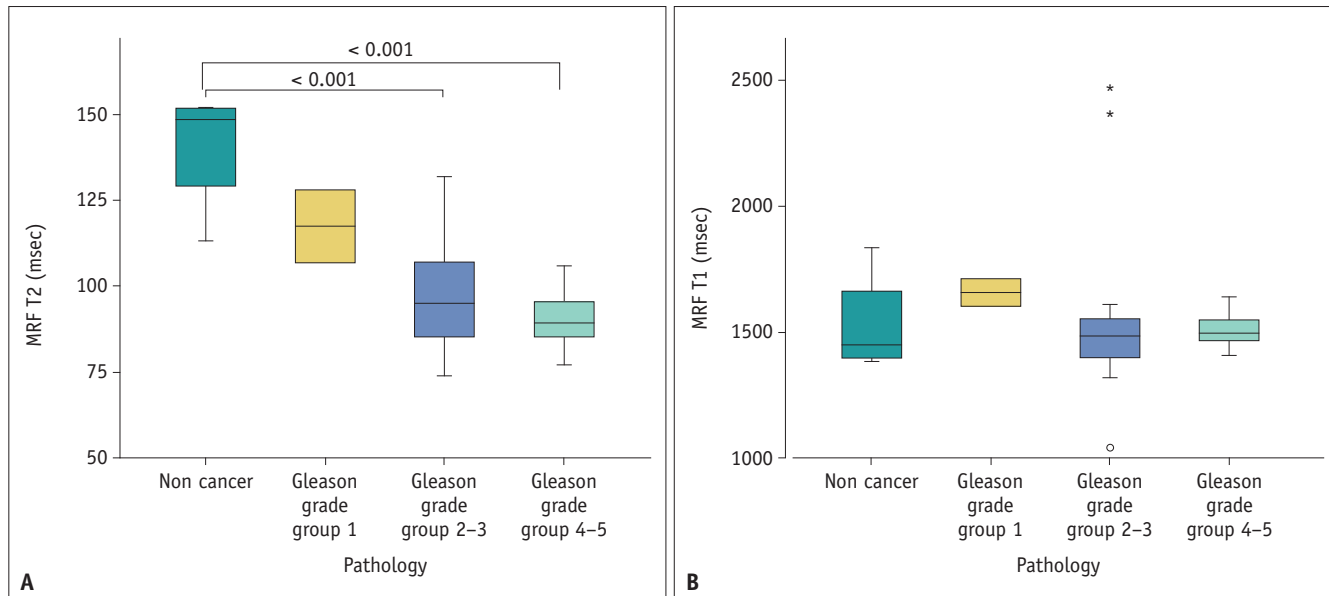
Fig. 4. Differences in MRF-derived T1 and T2 values according to the pathology results.
A, B. The graph shows that the higher the cancer grade, the lower the T2 value **(A)**. The T2 value in non-cancerous lesions was significantly higher than that in Gleason grades 2–3 and 4–5 lesions. There was no significant difference in T1 values according to the pathology results **(B)**. MRF = MR fingerprinting

values were 169 and 65 ms in the peripheral and transition zones, respectively [10,12]. Although other studies have reported T1 and T2 values in the prostate gland, the values in the peripheral and transition zones were not separately analyzed [18-20]. Therefore, the similarity of the values between studies is difficult to evaluate. The differences in results may be due to the differences in the image analysis method; most studies used a small circular ROI to measure the values in normal prostate tissues. We selected a section and drew an ROI to cover the entire visually normal tissue in that section. Different MRI techniques may also cause differences in T1 and T2 values. However, higher T1 and T2 values in the peripheral zone than in the transitional zone were commonly reported in all studies.

We conducted a phantom study to verify the accuracy of MRF-derived T1 and T2 values. For the gold standard, conventional T1 and T2 mapping methods were obtained for more than 3 hours, and their values were set as target values. Even though there was a small, constant difference between the target and measured T1 and T2 values, the measured T1 and T2 values were significantly correlated with the target values (R = 0.99979 and 0.99810, respectively). Therefore, the phantom study proved the reliability of the MRF results. We believe that MRF would also be reliable in a clinical study, since the same MRF protocols were used in both the phantom and clinical studies [10-13].

In this study, we used a new 3D MRF technique that can obtain images in less than 4 minutes. The advantages of the new MRF technique, along with the short acquisition time, include higher spatial resolution (0.6 x 0.6 mm) and smaller thickness (3 mm) than the previously used MRF technique (1 x 1 x 5 mm) [10-13]. The margin of the focal lesion was well-defined on high-resolution images. The resolution and thickness of the MRF and T2WI were equally set in our study. Therefore, evaluating MRF with reference to T2WI is easy, since the same section is obtained with the same thickness. Using a 3D image acquisition technique has several benefits in conventional MRI such as: 1) smaller slice thickness, 2) the signal-to-noise ratio is higher than that in 2D acquisition, and 3) additional acceleration in the z direction is possible. 3D MRF in a small organ like the prostate gland, may be advantageous due to the reduction of slice thickness and reconstruction of multiplanar images.

This study has several limitations. First, only a small number of patients were diagnosed with prostate cancer hence, the differences in T1 and T2 values between normal tissue and prostate focal lesions were analyzed in only 29 patients. The main purpose of this study was to explore the feasibility of the new 3D MRF technique in clinical practice. We showed the preliminary results of prostate cancer on MRF images, and further study is recommended. Second, we did not divide the prostate cancer lesions according to their location in the peripheral or transition zone. In previous studies of prostate MRF, some differences were found in the

REFERENCES

1. Ahmed HU, El-Shater Bosaily A, Brown LC, Gabe R, Kaplan R, Parmar MK, et al. Diagnostic accuracy of multi-parametric MRI and TRUS biopsy in prostate cancer (PROMIS): a paired validating confirmatory study. *Lancet* 2017;389:815-822

2. Kasivisvanathan V, Rannikko AS, Borghi M, Panebianco V, Mynderse LA, Vaarala MH, et al. MRI-targeted or standard biopsy for prostate-cancer diagnosis. *N Engl J Med* 2018;378:1767-1777

3. Baur ADJ, Hansen CM, Rogasch J, Posch H, Elezkurtaj S, Maxeiner A, et al. Evaluation of T1 relaxation time in prostate cancer and benign prostate tissue using a Modified Look-Locker inversion recovery sequence. *Sci Rep* 2020;10:3121

4. Mai J, Abubrig M, Lehmann T, Hilbert T, Weiland E, Grimm MO, et al. T2 mapping in prostate cancer. *Invest Radiol* 2019;54:146-152

5. Chatterjee A, Devaraj A, Mathew M, Szasz T, Antic T, Karczmar GS, et al. Performance of T2 maps in the detection of prostate cancer. *Acad Radiol* 2019;26:15-21

6. Foltz WD, Haider MA, Chung P, Bayley A, Catton C, Ramanan V, et al. Prostate T(1) quantification using a magnetization-prepared spiral technique. *J Magn Reson Imaging* 2011;33:474-481

7. Wu LM, Chen XX, Xuan HQ, Liu Q, Suo ST, Hu J, et al. Feasibility and preliminary experience of quantitative T2* mapping at 3.0 T for detection and assessment of aggressiveness of prostate cancer. *Acad Radiol* 2014;21:1020-1026

8. Ma D, Gulani V, Seiberlich N, Liu K, Sunshine JL, Duerk JL, et al. Magnetic resonance fingerprinting. *Nature* 2013;495:187-192

9. van Houdt PJ, Agarwal HK, van Buuren LD, Heijmink SWTPJ, Haack S, van der Poel HG, et al. Performance of a fast and high-resolution multi-echo spin-echo sequence for prostate T2 mapping across multiple systems. *Magn Reson Med* 2018;79:1586-1594

10. Panda A, Obmann VC, Lo WC, Margevicius S, Jiang Y, Schluchter M, et al. MR fingerprinting and ADC mapping for characterization of lesions in the transition zone of the prostate gland. *Radiology* 2019;292:685-694

11. Panda A, O'Connor G, Lo WC, Jiang Y, Margevicius S, Schluchter M, et al. Targeted biopsy validation of peripheral zone prostate cancer characterization with MR fingerprinting and diffusion mapping. *Invest Radiol* 2019;54:485-493

12. Yu AC, Badve C, Ponsky LE, Pahwa S, Dastmalchian S, Rogers M, et al. Development of a combined MR fingerprinting and diffusion examination for prostate cancer. *Radiology* 2017;283:729-738

13. Shiradkar R, Panda A, Leo P, Janowczyk A, Farre X, Janaki N, et al. T1 and T2 MR fingerprinting measurements of prostate cancer and prostatitis correlate with deep learning-derived estimates of epithelium, lumen, and stromal composition on corresponding whole mount histopathology. *Eur Radiol*

results according to cancer location. Studies that evaluate the differences between transition zone and peripheral zone cancers should be conducted. Third, volumetric analysis was not performed. Volumetric analysis can correct the bias by selecting specific areas for small ROIs. Instead, we used ROIs that covered the entire area of the selected section. Although this technique is limited compared to volumetric analysis, we believe that it is a more objective method than the small ROI method.

In conclusion, the T1 and T2 values obtained from 3D MRF showed a perfect correlation with the gold standard values in the phantom study. Differences in the T1 and T2 values among the different zones of the prostate gland were identified using 3D MRF in patients.

Supplement

The Supplement is available with this article at https://doi.org/10.3348/kjr.2020.1362.

ORCID iDs

Dongyeob Han
  https://orcid.org/0000-0002-1402-5036
Moon Hyung Choi
  https://orcid.org/0000-0001-5962-4772
Young Joon Lee
  https://orcid.org/0000-0001-8309-0272
Dong-Hyun Kim
  https://orcid.org/0000-0002-6717-7770

2021;31:1336-1346

14. Ma D, Jones SE, Deshmane A, Sakaie K, Pierre EY, Larvie M, et al. Development of high-resolution 3D MR fingerprinting for detection and characterization of epileptic lesions. *J Magn Reson Imaging* 2019;49:1333-1346

15. Yushkevich PA, Piven J, Hazlett HC, Smith RG, Ho S, Gee JC, et al. User-guided 3D active contour segmentation of anatomical structures: significantly improved efficiency and reliability. *Neuroimage* 2006;31:1116-1128

16. Liu W, Turkbey B, Sénégas J, Remmele S, Xu S, Kruecker J, et al. Accelerated T2 mapping for characterization of prostate cancer. *Magn Reson Med* 2011;65:1400-1406

17. Simpkin CJ, Morgan VA, Giles SL, Riches SF, Parker C, deSouza NM. Relationship between T2 relaxation and apparent diffusion coefficient in malignant and non-malignant prostate regions and the effect of peripheral zone fractional volume. *Br J Radiol* 2013;86:20120469

18. Bojorquez JZ, Bricq S, Acquitter C, Brunotte F, Walker PM, Lalande A. What are normal relaxation times of tissues at 3 T? *Magn Reson Imaging* 2017;35:69-80

19. Bojorquez JZ, Bricq S, Brunotte F, Walker PM, Lalande A. A novel alternative to classify tissues from T 1 and T 2 relaxation times for prostate MRI. *MAGMA* 2016;29:777-788

20. de Bazelaire CM, Duhamel GD, Rofsky NM, Alsop DC. MR imaging relaxation times of abdominal and pelvic tissues measured in vivo at 3.0 T: preliminary results. *Radiology* 2004;230:652-659